# Impedance Spectroscopic Detection of Binding and Reactions in Acid-Labile Dielectric Polymers for Biosensor Applications

| | |
|---|---|
| Journal: | *Journal of Materials Chemistry B* |
| Manuscript ID | TB-COM-12-2017-003171.R1 |
| Article Type: | Communication |
| Date Submitted by the Author: | 05-Apr-2018 |
| Complete List of Authors: | Dailey, Jennifer; Johns Hopkins University, Materials Science and Engineering<br>Fichera, Michelangelo; Johns Hopkins University, Materials Science and Engineering<br>Silbergeld, Ellen; Johns Hopkins University Bloomberg School of Public Health, Environmental Health and Engineering<br>Katz, Howard; Johns Hopkins University, Materials Science and Engineering |
| | |

# Impedance Spectroscopic Detection of Binding and Reactions in Acid-Labile Dielectric Polymers for Biosensor Applications

Jennifer Dailey[1], Michelangelo Fichera[1], Ellen Silbergeld[2], Howard Katz[1]

[1] Department of Materials Science and Engineering, Whiting School of Engineering, Johns Hopkins University

[2] Department of Environmental Engineering, School of Public Health, Johns Hopkins University

**Abstract:**

We synthesized previously unreported copolymers with cleavable acid-labile side chains for use as electrochemical sensing layers in order to demonstrate a novel architecture for a one-step immunosensor. This one-step system is in contrast to most antigen-capture signal amplification methods which involve complicated secondary labeling techniques, or require the addition of redox probes to achieve a sensing response. A series of novel copolymers composed of various trityl-containing monomers were synthesized and characterized to determine their dielectric properties. Results indicate that the thin films of these polymers are stable in water, but some begin to degrade under acidic conditions or upon antigen binding, causing observable changes in the phase angle.

## 1. Introduction

Electrochemical impedance spectroscopy (EIS) offers an attractive solution to development of fast, point-of-care sensors for detecting specific molecules in biological samples[1–4]. The development of a diagnostic system that requires only minutes to complete a sample analysis with an electronic readout could lead to major improvements in prevention and therapy in healthcare settings and increased reliability of food safety.[5–7] We address this latter goal by our choice of a Penicillin binding protein 2a (PBP2a) as a test analyte for EIS studies as described below. This protein is an indicator of methicillin resistant *Staphylococcus aureus* (MRSA), a high priority pathogen for both human health and food safety.[8–11]

Over the past few decades, many researchers have made great strides in increasing the sensitivity of the EIS method of detection through alteration of electrodes, miniaturization and multiplexing, use of different binding materials, and various forms of labelling.[3,12–15] However, a single molecular binding event would be expected to produce minimal resistive or capacitive change in an impedimetric system, limiting our ability to detect low levels of analyte in normal human samples that are composed of an extensive mixture of different proteins. Labelling systems, such as the addition of secondary enzymes in a classic enzyme-linked immunosorbent assay (ELISA) geometry, have been shown to drastically increase sensitivity by causing further electronic interactions at the interface, and they could be an ideal solution to diagnostic sensors in environments with trained technical personnel.[16,17] Unfortunately, the addition of labelling to the EIS system creates extra steps that both complicate use of the system and may be a source of increased errors due to improper or insufficient sample washing. Classical faradaic EIS detection methods use redox probes in order to measure charge transfer across a sensing layer, but this also requires some sample processing in order to add the probe. Nonfaradaic EIS detection systems use the same device architecture with different assumptions of mechanism of action, and rely primarily on changes in capacitive properties of the film being measured, and these require no redox probes.[18] With this motivation, for the purposes of creating a sensor that is truly one-step, we focus on designing a more responsive, polymer-based analyte binding layer, and we avoid any secondary binding steps by measuring and analyzing the nonfaradaic response.

A sensor based on EIS detection of the degradation of a polymer layer is a concept that has already been reported for enzyme-substrate systems, and the capacitive effect of the general degra-

dation phenomenon has been additionally well studied in paint coatings on metals[19–22]. Particularly effective are films composed of enzymatically cleavable bonds that indicate the presence of even a small amount of enzyme in solution. In order to increase the limited signal produced by a single binding interaction of noncatalytic antibody and antigen, we have created and characterized a novel polymer structure with fragile, degradable side chains. The alteration of the polymer dielectric layer upon analyte attachment produces an increased signal compared to the effect of a typical binding event. To the best of the authors' knowledge, this is the first time that EIS has been used to detect polymer degradation based on a label-free antibody-antigen binding event.

The key chemical features in our polymers are trityl-based groups, including unsubstituted trityl, 4-monomethoxytrityl (MMT), and (4,4)-dimethoxytrityl (DMT), which have long been used to protect hydroxyl groups from undesired reaction during chemical transformations of accompanying functional groups. DMT can be very easily removed with weak acid ("deprotected"), making it a favorite protecting group during synthesis. The use of trityl-based groups in polymers has been studied, and their bulkiness compared to the carbon backbone can produce isotropic chains as the monomers are forced into restricted spaces around the steric bulk.[23–25] Due to their fragility, these protecting groups are typically meant as intermediaries in the synthesis of another compound, and are not the final product. Homopolymers of the trityl methacrylate groups are extremely insoluble in standard solvents. Because our group obtained utility from poly(benzyl methacrylate) as a thin film dielectric layer for sensing purposes, we chose to create a series of trityl copolymers incorporating benzyl methacrylate and the various trityl methacrylates.[26]

These previously unreported polymers were extensively characterized using NMR and gel permeation chromatography (GPC), and their thin film layers were tested for their dielectric properties. The free volume around the trityl groups can allow for increased free rotation of polar and polarizable functional groups of the polymer, which would increase the dielectric constant, k. Additionally, if this volume becomes filled with a polar solvent such as water (k=~80), there will be a significant change in EIS measurements.[27] A stable dielectric layer for an aqueous EIS system, which is not our main goal here, must be impermeable to water, since absorption of water into the film would drastically change its capacitive effects. Just as benzyl methacrylate is completely insoluble in water and produces a stable film, out trityl copolymers in their pristine form are similarly hydrophobic. However, as the trityl groups begin to deprotect, water is allowed to enter the film, furnishing an additional mechanism for electronic signaling.

For all analyte sensing measurements in this work, we used a polymer blend of the trityl copolymer and a polymer composed of benzyl methacrylate and methacrylic acid groups. These acid groups were used to covalently bind antibodies to the polymer thin film in very close proximity to the trityl side chains, using standard carbodiimide crosslinking chemistry, which has been well-established as an effective tool for immunosensor fabrication[28–32].

## 2. Materials and Methods

2.1 Source Materials

Glass slides were purchased from Corning and thoroughly cleaned before use as described below. A 1mL three-probe impedance testing cell was purchased from CH Instruments Inc (Texas). MRSA antibodies corresponding to PBP2a were purchased from Abnova. FITC-tagged glial fibrillar acidic protein (GFAP) antibody was purchased from EMD Millipore. All

other chemicals were purchased from Sigma, in anhydrous condition if possible, and were not additionally purified before use. Synthesized monomers and polymers were analyzed using NMR to confirm composition (SI 2). A PARSTAT 2273 was used to take EIS measurements and controlled with PowerSuite software. An Olympus IX71 was used to take fluorescent images.

2.2 Substrate Preparation

Corning glass was cut into 1' squares and cleaned by liquid soap and water, followed by sonication for 15 minutes in both acetone and isopropanol. The glass substrates were dried with nitrogen flow and immediately deposited with Cr/Au (5nm/50nm) at $<6 \times 10^{-6}$ Torr using thermal evaporation. Substrates were kept under vacuum until use.

2.3 Trityl-based Monomer synthesis:

Trityl methacrylate (TrM) was synthesized according to Yuki (summarized in Scheme 1), with minor adjustments[24]. Briefly, methacrylic acid was added to a sealed flask of toluene cooled in an ice bath, and triethylamine was added thereto. Trityl chloride was dissolved in a small amount of toluene and injected into the system, while under nitrogen. The mixture was allowed to stir for two hours, and the precipitated salt was filtered away. The mixture was then held at -5°C overnight, at which point additional salt precipitated and was filtered. The remaining solvent was evaporated and the monomer was recrystallized from diethyl ether, producing large, white crystals resembling granulated sugar.

Monomethoxytrityl methacrylate (MMTM) was synthesized similarly as above using monomethoxytrityl chloride as the precursor. As this reaction progressed far more slowly due to the additional methoxy group, TLC (DCM:DMF 1:1) was used to confirm that the starting

products were converted at various time intervals.  The reaction was allowed to continue for three hours, and the precipitated salt was filtered away.  The monomer was washed three times with saturated aqueous sodium bicarbonate and dried over sodium sulfate.  The remaining organic layer was evaporated away under vacuum, resulting in a viscous, pale yellow oil.

Dimethoxytrityl methacrylate (DMTM) was synthesized in the same manner as MMTM, using dimethoxytrityl chloride as precursor, resulting in a viscous, yellow oil.  Trimethoxytrityl methacrylate (TMTM) was also synthesized as above, but was found to be so labile during washing that no significant quantity of desired product could survive to polymerization. Trimethoxytrityl is mentioned in the literature as being overly cleavable for practical use.[33]

2.4 Polymer Synthesis:

Copolymerization of all monomers and methacrylic acid with benzyl methacrylate (mixed in equimolar ratio) was accomplished through free-radical polymerization using azobisisobutyronitrile (AIBN) as initiator under anhydrous conditions in nitrogen, summarized in Scheme 2.  Polymer was precipitated in hexane cooled below room temperature with an ice bath, and any unreacted monomers were removed in warm toluene.   With the exception of the simple copolymer of methacrylic acid and benzyl methacrylate, these trityl-based polymers did not dissolve fully in most solvents.  Only anisole and dimethylformamide (DMF) were found to be suitable candidates [See Table 1].  Polymers were dissolved at a concentration of 50 mg/ml and filtered through a 0.45 um syringe filter.  Polymer films were created through spincasting of solutions on prepared substrates at a speed of 1500 rpm for 60 seconds in an inert nitrogen atmosphere.   Samples were annealed at 60°C for one hour under nitrogen to remove any excess solvent.

Scheme 1



Scheme 2



Where R=  H  OR    OR  

OR    OR  
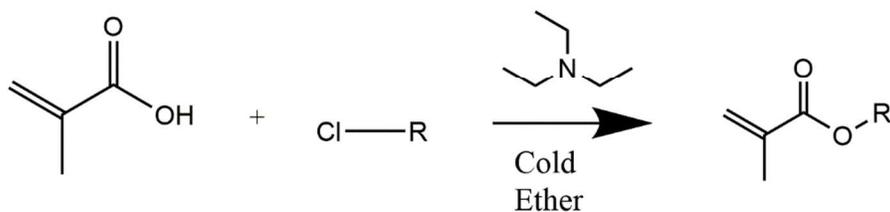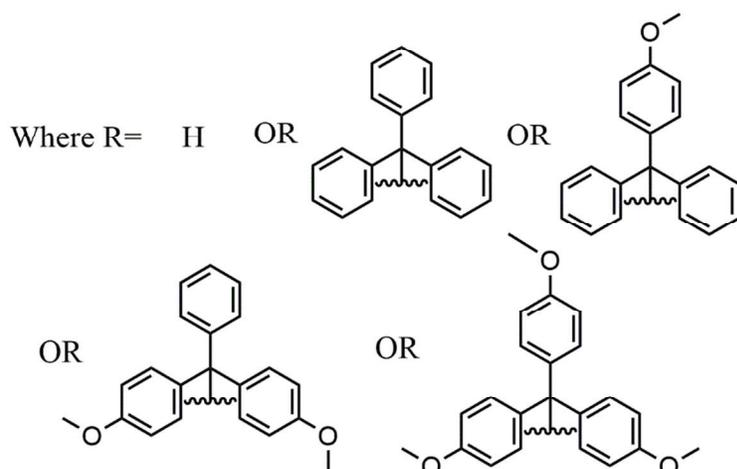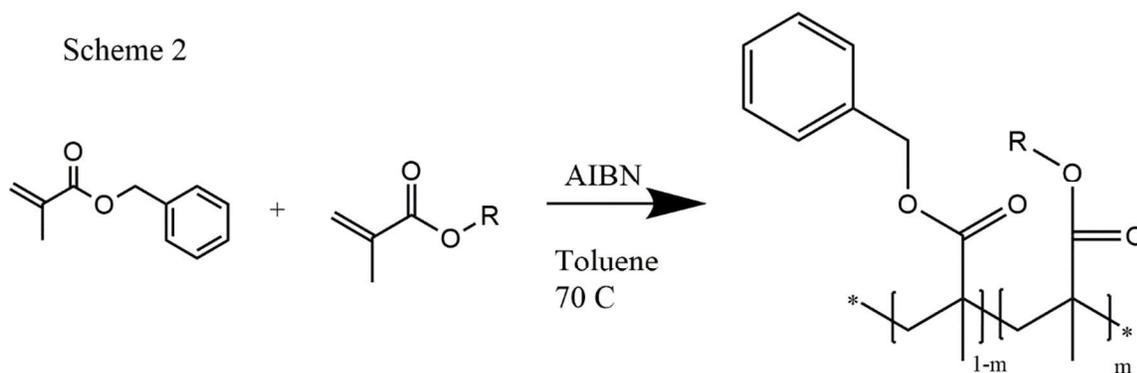
## 2.5 Antibody Deposition:

Benzyl methacrylate-co-methacrylic acid polymer (polyBMMA) was activated and attached to MRSA or GFAP antibodies through standard carbodiimide chemistry. Polymer was dissolved in DCM/DMF (1:4) at a concentration of 10 mg/ml. 30 mg/ml 1-ethyl-3-(3-dimethylaminopropyl)carbodiimide hydrochloride (EDC) was added thereto and vortex-mixed

for one hour. 15 mg/ml N-hydroxysuccinimide (NHS) was added thereto and allowed to mix an additional two hours. The EDC/NHS-activated polymer solution was filtered through a 0.45um syringe filter and mixed with polyDTMB (80mg/ml in DCM) at a 1:1 ratio to produce a polymer blend. This was deposited as described previously, and subsequently washed with DI water to remove any excess EDC/NHS. MRSA antibody at a concentration of 1 mg/ml was incubated on the film for twelve hours in a humid container to avoid evaporation. Samples were washed three times with DI water. Bovine serum albumin (BSA, 1 mg/ml) was deposited and allowed to react for 1 hour to passify any remaining activation sites. The substrates were washed three additional times with DI water and promptly characterized.

FITC-tagged anti-GFAP (glial fibrillary acidic protein) antibody was also deposited as described above on a clean plain glass substrate covered in activated polymer blend and assayed with a fluorescent microscope to ensure selective antibody attachment. This was compared to a non-EDC/NHS treated polymer blend of the same composition exposed to fluorescent antibody.

2.6 pH exposure:

PBS buffer was adjusted to various pH using dilute HCl or NaOH as applicable. Buffer was dropped onto prepared films and incubated for one hour in a humid environment to avoid evaporation, then dried under nitrogen flow.

2.7 EIS Measurements:

The fabricated polymer film samples served as working electrodes and were placed into the testing cell under an O-ring. Alligator clips were attached to a cleaned gold portion of the glass slide, the top portion of the coil platinum counter electrode, and the Ag/AgCl reference electrode.

Measurements were taken at 100 mV and a frequency of 1 Hz to 500 KHz. All measurements and attachment procedures were completed at room temperature over the course of tens of minutes, since this device is designed for extremely simple use in such conditions.

## 3. Results

### 3.1 Polymer Synthesis

Polymerization stopping time was determined by intermittently taking a few drops from the reaction flask via syringe and observing whether a precipitate formed when dropped into one mL of cold hexane. Once precipitation occurred, the reaction flask was cooled to stop further polymerization and purified to remove unreacted monomer through subsequent precipitation in cold hexane followed by washing in warmed toluene. Percent of active group attachment was determined by NMR and Mn was determined by GPC (SI 1) as shown in the graph (Table 1). Both indicate the successful inclusion of the trityl-based protecting groups into the polymer chain. (4,4,4)-trimethoxytrityl (TMT) was briefly studied in this work, but as others have found, its carbocation appeared to form and become substituted so readily that it was unstable in any of our attempted syntheses. Resulting polymers were generally not soluble in most generally used solvents, as has been observed by previous groups. Solvents found to be successful for casting each polymer are listed in Table 1.

*Table 1 Characterization of all polymers formed, based on NMR and GPC measurements. % Trityl Monomer successfully polymerized refers to the final polymer percentage, as calculated from NMR, though the original molar concentrations between monomers were 1:1.*

| Active Group | Monomer/co-Polymer Abbreviation | AIBN added (mol equiv.) | Time (days) | % Trityl Monomer Successfully Polymerized | Mn | Suitable Solvent |
|---|---|---|---|---|---|---|
| Methacrylic acid | MA/pBMMA | .02 | 1 | 25 | 10000 | Various |
| Trityl methacrylate | TrM/pBMTrM | .04 | 4 | 25 | 12500 | Anisole |
| Monomethoxytrityl methacrylate | MTrM/pBMMTrM | .08 | 7 | 40 | 7700 | DMF |
| Dimethoxytrityl methacrylate | DTrM/pBMDTrM | .08 | 7 | 10 | 23000 | DMF |
| Trismethoxytrityl methacrylate | TMTrM/pBMTMTrM | .08 | 9 | N/A | N/A | N/A |

3.2 Dielectric characterization

Polymers were cast into thin films on gold electrodes as described and dielectric constant of each polymer type was measured using a two-probe sandwich capacitor according to the formula:

$$C = \frac{\kappa \varepsilon_0 A}{d}$$

Where C is our measured capacitance, k the dielectric constant, $\epsilon_0$ the permittivity of vacuum, A the area covered by our indium-gallium coated top probe tip, and d the height of our thin film measured by laser microscopy and averaged for each sample type. D, the dissipation constant, was also measured. D is a measure of the amount of energy lost as heat through the system when AC voltage is applied. It is higher in imperfect films containing holes and conductive pathways, and dielectrics considered useful in industry typically have a D < 0.05 or lower. Results for each measured benzyl methacrylate co polymer type are shown in Table 2.

*Table 2 Dielectric constant and K values of polymer films, as calculated using capacitive and height measurements.*

|  | PolyBMTrM | PolyBMMTrM | PolyBMDTrM |
|---|---|---|---|
| K: | 4.00 4.04 | | 4.31 |
| D: | 0.03 0.13 | | 0.05 |

PMMA has a dielectric constant of 3-5, making these results reasonable for methacrylic polymer thin films. The somewhat higher dielectric constants for the larger side chains are understandable, since the methoxy groups are adding bulky side groups to the system and a small amount of polarity, both of which would contribute to the increase in k, assuming the side groups maintain some degree of rotational freedom.

3.3 Film dissolution under acidic pH conditions
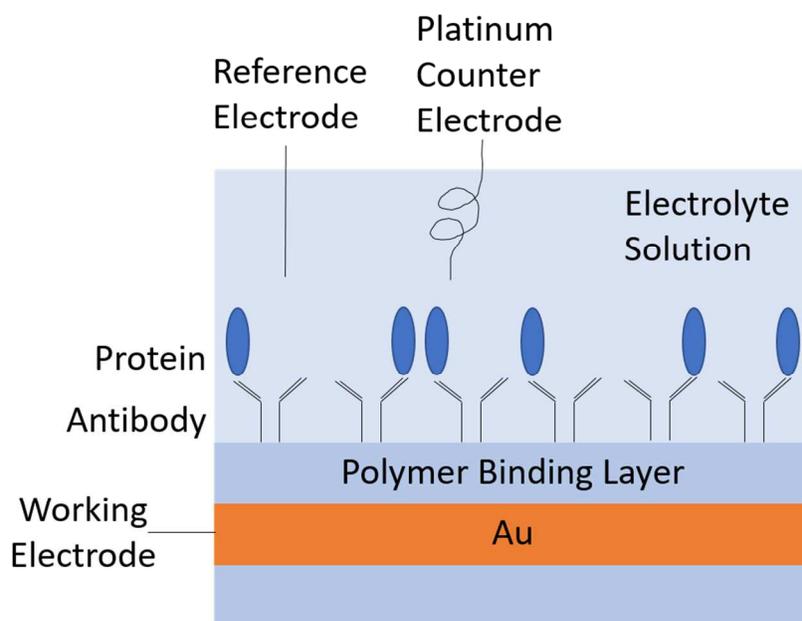


*Figure 1 Schematic of standard EIS system using reference, working, and counter electrodes in a PBS electrolyte solution.*

A typical three-probe EIS system is composed of working, counter, and reference electrodes (Figure 1). The working electrode supports the dielectric polymer on which the binding sites for our target of interest are located, and the counter electrode is a coiled, inert platinum rod, set to the voltage of the reference electrode, with sufficient surface area so as not to be the limit of charge transfer in the system. The counter and reference electrodes are placed in a solution that covers the totality of the working electrode, and a small AC voltage over a range of frequencies is applied between the working and reference/counter electrodes. Any alteration in working electrode resistance or capacitance will be read on the Nyquist and Bode output graphs as parts of the real and imaginary impedance. Each measurement takes less than two minutes to run through all frequencies, making each experiment (including a run to check for stability) <1 hour in duration.

Films of each polymer were cast onto cleaned glass substrates and incubated with acidic solutions. Complex impedance changes are shown in Figures 2a-c. Sample topologies were characterized qualitatively using differential interference contrast (DIC) microscopy in order to view any large-scale morphological changes in film quality following acid exposure (Figure 2d).
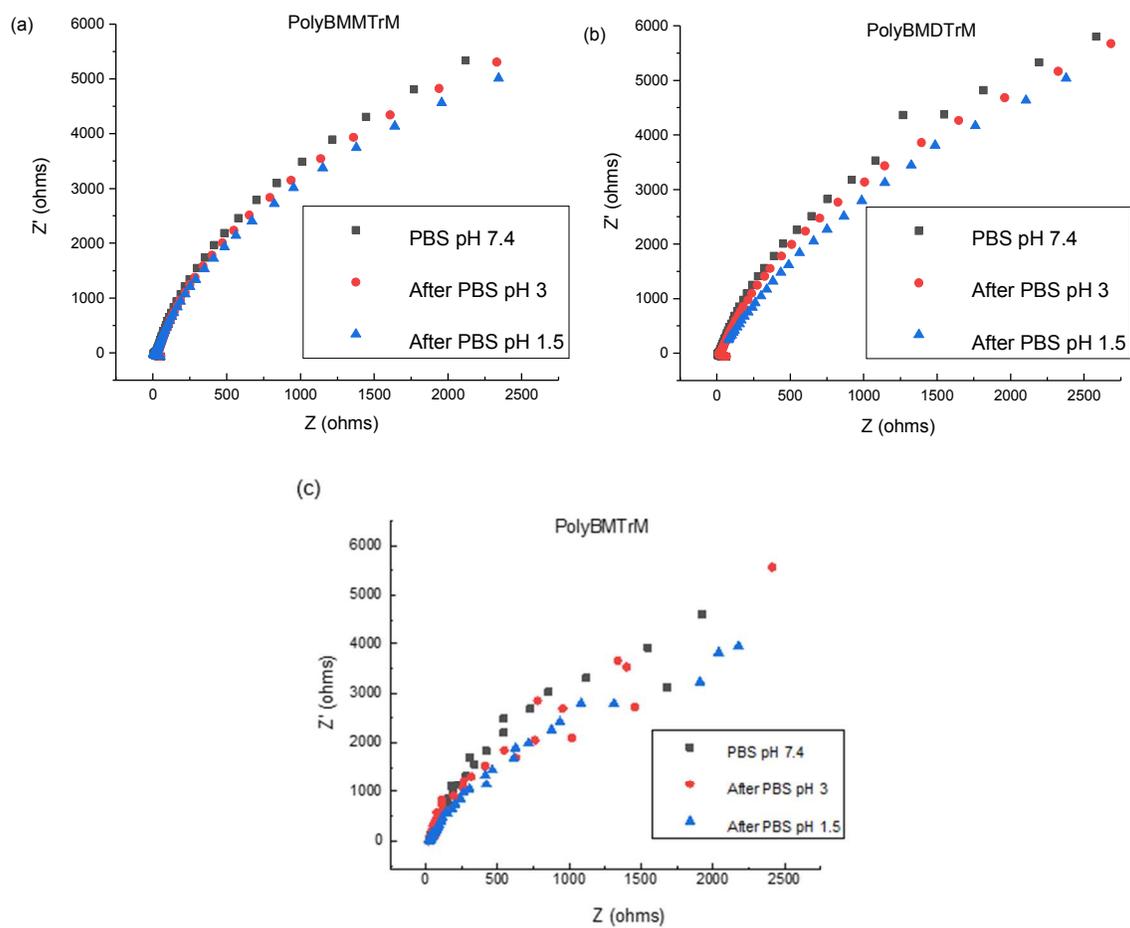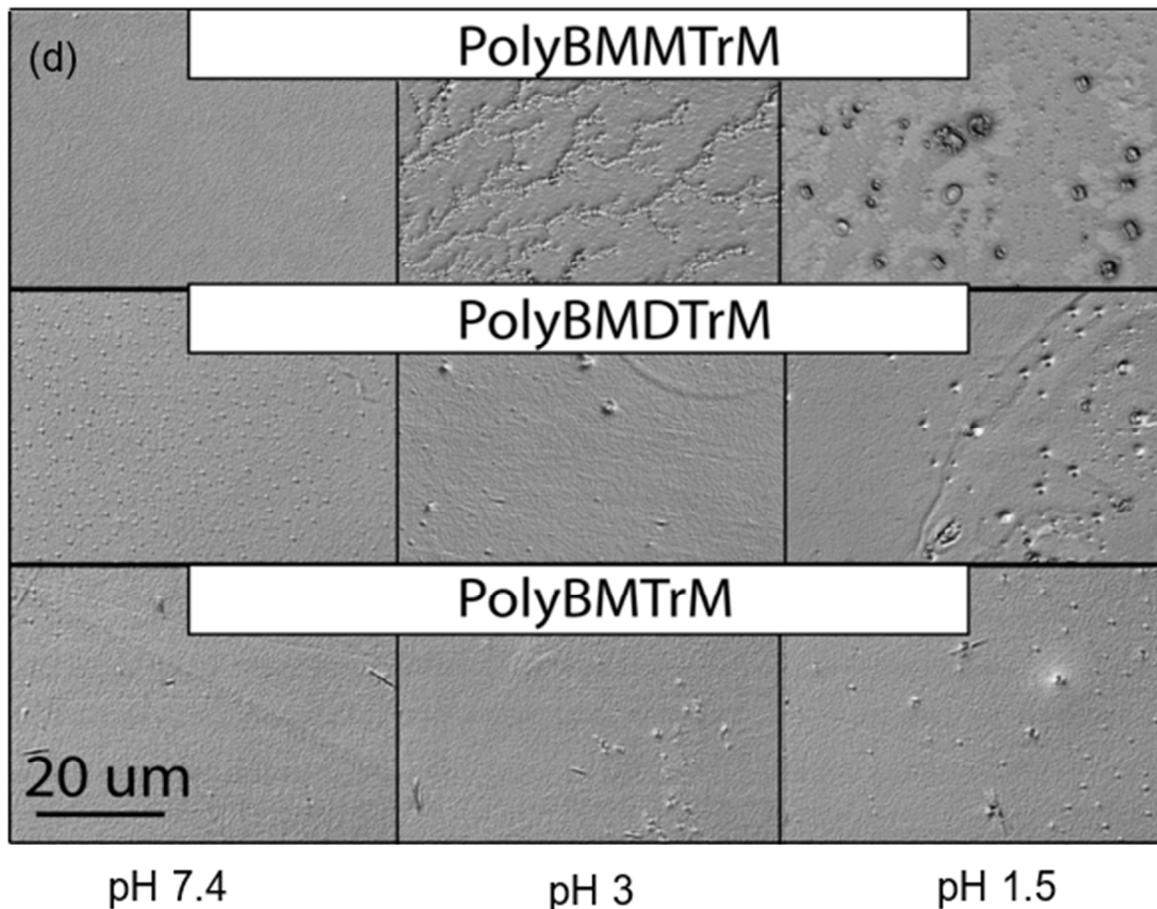
*Figure 2 (a-c)) show response of each type of polymer film to various acidity levels on standard Nyquist plots. (d) shows DIC images of each type of polymer after it was allowed to react with PBS solutions of different acidities.*

Under optimal spincasting conditions as described in Materials and Methods, the films appear clean and flat under 100X zoom. After incubation with standard PBS (pH 7.4), the films show no visible degradation (left column) and the polymer films remain similar in appearance. Under mildly acidic pH conditions (PBS at pH 3 incubated for one hour, middle column), film degradation becomes somewhat apparent. The monomethoxytrityl-based polymer developed tendril structures that are likely precipitation of the monomethoxytrityl group having cleaved

from the polymer chain at this mildly acidic pH. The dimethoxytrityl-based polymer begins to show some larger hills and valleys, and the trityl-based polymer has similar pin-hole features.

Following an hour incubation with more acidic PBS (pH 1.5, right column), larger and more extensive features were noticed in all three polymer films. The monomethoxytrityl and dimethoxy-based polymers both developed much larger holes throughout the film. The trityl-based polymer had more pinholes, but they were not of comparable size compared to what was found in the methoxylated materials. As the monomethoxytrityl group was able to polymerize at a much higher ratio in the polymer, it is presumed that the impact of so many bulky, fragile protecting groups has a very significant impact on the stability of the polymer in acidic environments. While the dimethoxytrityl group was not as easily incorporated into polymer under similar conditions, the second methoxy group makes this a more fragile protecting group that should deprotect significantly faster than other trityl-based groups, according to the literature. The loss of such bulky side chains would be expected to cause rearrangement of the otherwise stable polymer and result in such apparent film defects. The cleaved dimethoxytrityl group may exist as a more soluble species at this lower pH compared to what was observed at pH 3.

Films were additionally studied by EIS to see the combined resistive and capacitive effect of these morphological changes. To ensure measurement strictly of thin film change and ignore any effects caused by measuring in acidic solution, all measurements were taken in identical PBS (pH 7.4) buffer following incubation with the acidic PBS being measured. Due to the lack of significant morphological change seen with PolyBMTrM, as well as the literature indicating that this protecting group is significantly more stable than the others at anticipated pH's of interest, it

was deemed a poor candidate for use in a biosensor system where the pH will rarely deviate drastically.

Both mono- and dimethoxytrityl based polymers have a similar response to acidic pH as seen on the examples of typical Nyquist plots of Figures 2a-c, which corresponds to a small but regular shift in the phase component of the complex impedance, as indicated by the Nyquist plots having a decreased slope near our frequency of interest, 1 kHz for protein interaction studies described below.

### 3.3 Protein Response Studies

To determine whether antigen binding could result in a complex impedance change related to the acid-induced degradation observed above, we analyzed data taken by EIS with polymer exposure to neutral PBS buffer and added PBP2a antigen or control protein BSA.    Data were analyzed for phase shift at 1 kHz, a common frequency for measuring interactions occurring near the electrolyte interface rather than focusing on bulk or electrolyte properties.   After sweeping through the frequencies a minimum of three times to ensure stability in PBS, we injected protein solution ranging from 10 ng/ml to 1 ug/ml into the cell and measured the resulting change in complex impedance.

As demonstrated in the examples shown below, for both trityl-based and monomethoxytrityl-based polymers, we note either an increase in phase angle or small increase in overall resistance of the system following the addition of our protein of interest.  This is highly consistent with

many impedimetric biosensors that rely on additional coatings on the electrode surface (in this case, the attached protein) to increase charge transfer resistance in the system.[3] *PolyBMDTrM, on the other hand, showed consistent responses in the opposite direction.* In Figure (3d), we show data points indicating the resultant change in phase angle at 1 kHz caused by injection of varying concentrations of PBP2a, along with BSA (at a very concentrated 10 mg/ml). *The negative phase shift seen following all PBP2a injections is consistent with an increase in capacitance of the overall film system.* No significant change in resistance of the system was found at this frequency.



(a)

(b)

(c)
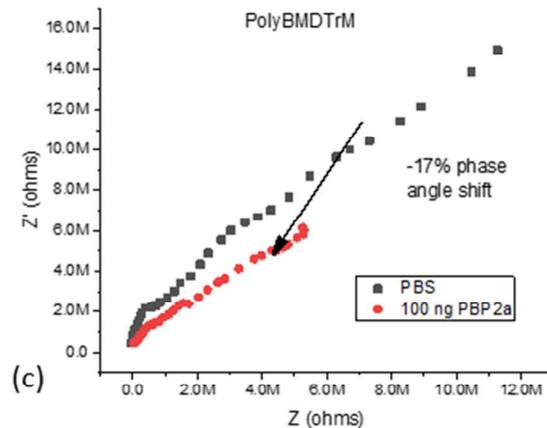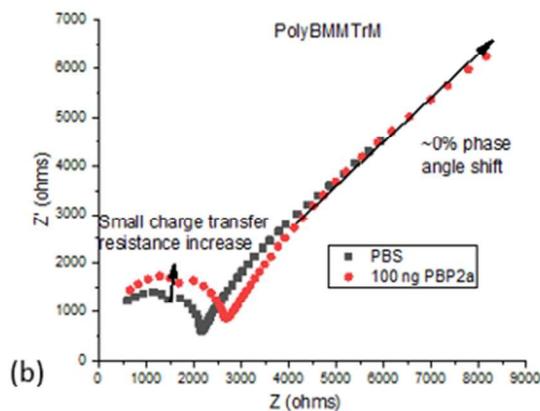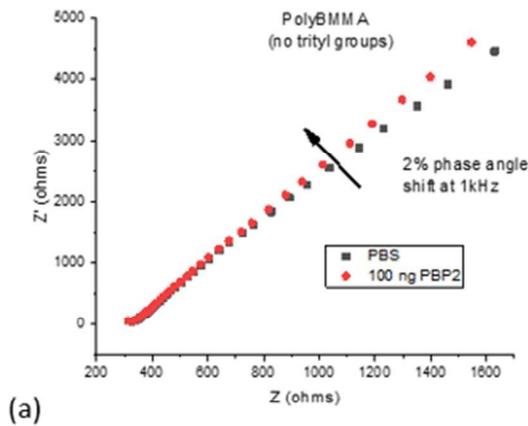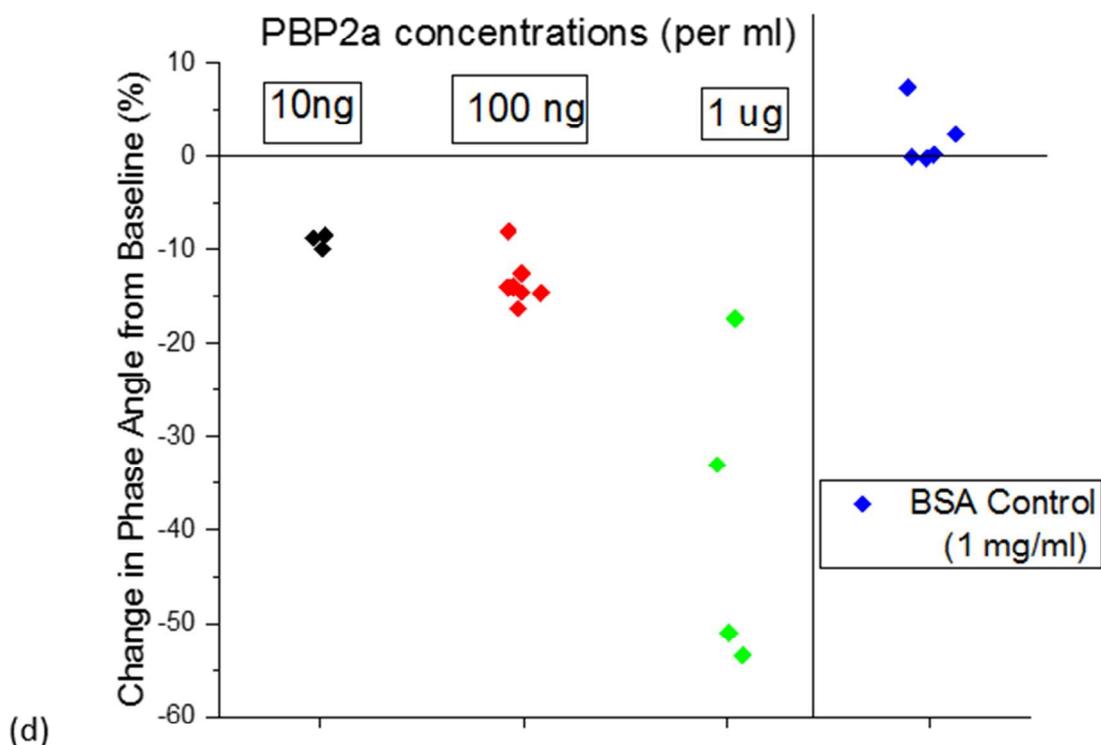
*Figure 3 (a)-(c) Demonstrate typical responses of each type of polymer reacting to protein binding. A polymer with no trityl groups (a) shows a small increase in phase angle corresponding to proteins attaching to the surface; (b) with monomethoxytrityl groups has a small increase in resistance as well. (c) Dimethoxytrityl groups result in a decrease in phase angle in response to protein attachment, with (d) displaying all results of PolyBMDTrM and, indicated on the right for comparison, performing a specificity check with high concentration bovine serum albumin (BSA) control.*

## 3.4 Antibody surface binding

As an additional test to ensure that our polymer films are both suitable for integration with biomolecules and will not be overly reactive to interfering species, we performed an antibody fluorescence experiment. Trityl-based co-polymers were blended with EDC-NHS activated polymers containing similar mole fractions of benzyl methacrylate groups to promote

homogeneity. A separate film was cast containing the same polymer blend without the EDC-NHS amine crosslinker molecules. Films were washed and incubated with a commercially-available FITC-tagged antibody to GFAP (as GFAP and PBP2a are both proteins with similar charge and size)[34]. FITC-tagged monoclonal antibodies corresponding to the same PBP2a epitope (amino acids 19-348) were not readily commercially available, but the anti-GFAP-antibody used in this experiment was also IgG1 from murine source, meaning the bulk of the antibody (including the heavy chain and amine group where our crosslinking chemistry of interest is taking place) was nearly identical except for the necessary fluorescent tag, making this product an appropriate  substitute to examine antibody-surface interaction. Following several washing steps to remove any unbound antibody, we took fluorescent images of both samples.

In Figure 4 (a), we see a very high amount of fluorescent activity, indicating very good attachment of GFAP antibody in the polymer blend. In (b), we see absolutely no green color, which means that there was no non-specific binding of antibody to our surface without EDC-NHS crosslinking chemistry. This indicates that our antibodies are covalently binding to their substrate as expected, and we do not have unreacted side chains causing unwanted attachment reactions to other moieties.
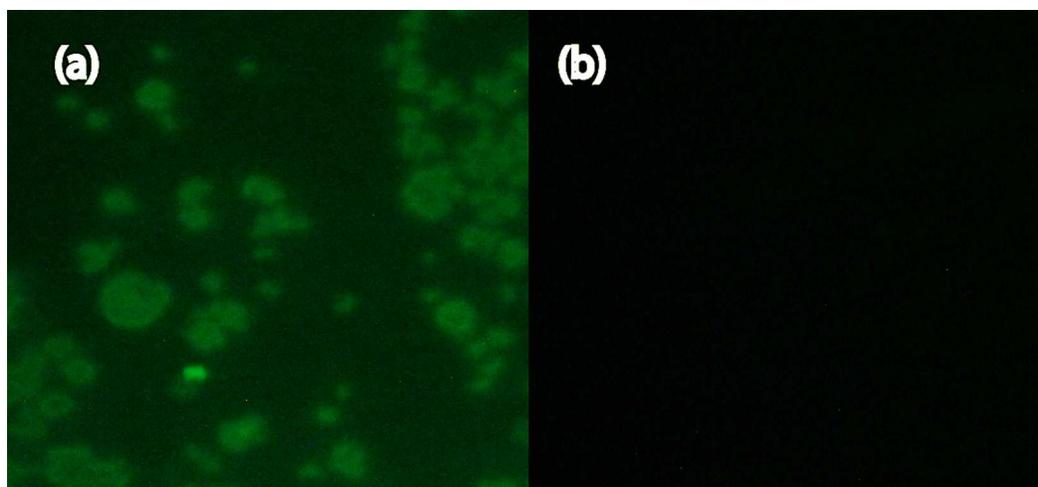
*Figure 4 (a) Shows FITC-tagged antibody on EDC-NHS activated polymer blend as shown by fluorescence microscopy. (b) No FITC-tagged antibody is present on unactivated polymer blend, indicating little non-specific binding to the surface. Brightness was increased 25% in both images to better display contrast*

## 4.  Discussion

Based on thin film characterizations showing impedimetric shifts upon short time period exposure to acidic pH as well as antigen, we propose two potential mechanisms of action by which this shift may be induced by the antigen, as shown in Figure 5.  Shown in the upper picture, as we have purposefully created a film with degradable side chains and have seen large holes in DIC images when films were exposed to acidic buffer for longer time periods (1 hour versus several minutes), there is the possibility that pin-holes are forming through the layer in response to protein attachment.  As the trityl side chains cleave, areas of the resulting film effectively become poly(methacrylic acid) (PMAA) which is more readily soluble in acidic aqueous solutions, compared to its protected counterpart.  In the lower picture, we show the possibility of changes in polymer structure allowing for sufficient molecular movement to allow water absorption through the formerly hydrophobic layer, though without visible pore formation.
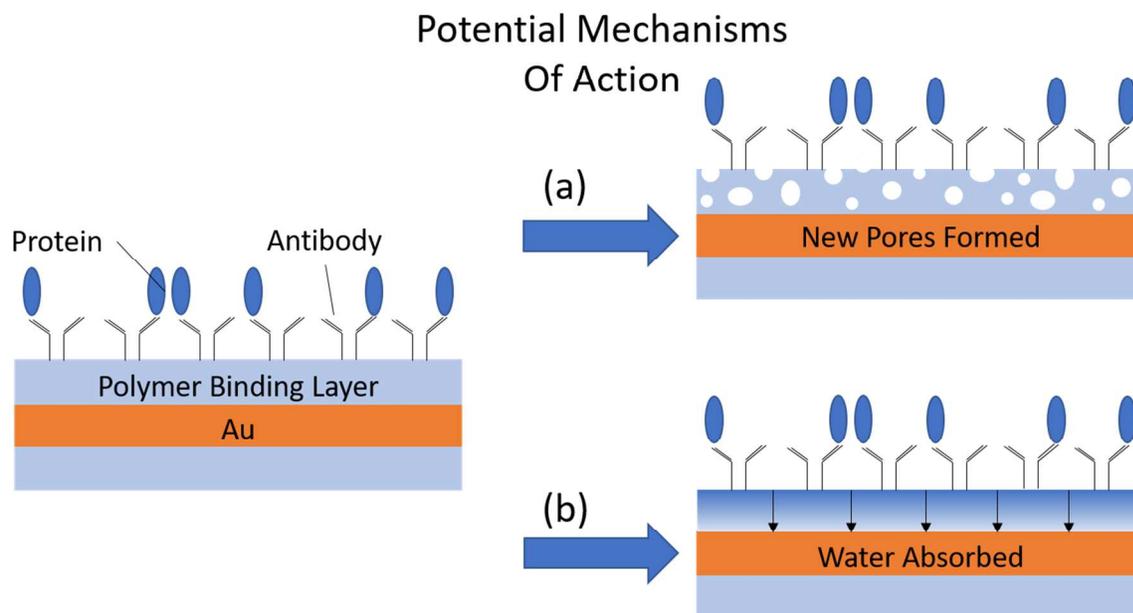
*Figure 5 Schematic displaying two potential mechanisms to explain EIS measurements. (a) indicates the formation of large holes through the film as seen in DIC, and (b) indicates gradual water absorption through the film as it becomes increasingly water soluble.*
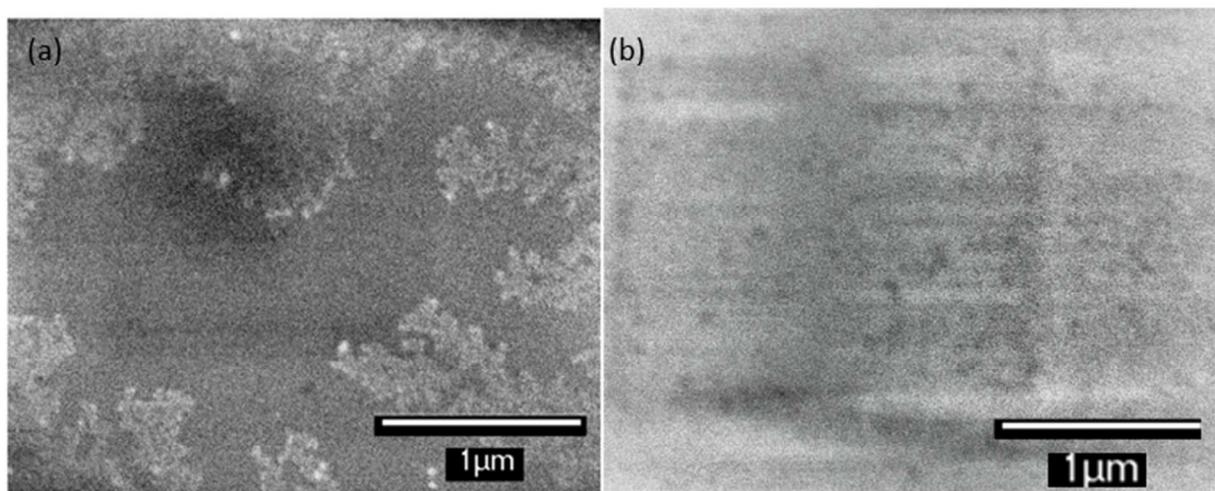


*Figure 6 SEM measurements of antibody attached on polymer blend surface before (a) and after (b) incubation with 100 µg/ml PBP2a protein.  In order to achieve sufficiently high signal, a 4 nm layer of platinum was sputter coated on top of the polymer films.  (a) Clearly shows defined regions of polymer segregation, as expected for a blend of this nature.  (b) lacks defined regions and additional begins to show small superficial pores in the range of nanometers, though the necessity of the platinum layer makes exact size difficult to interpret.*

While DIC measurements do indicate large pores forming at pH 1.5 in PBS buffer after one hour, we recognize that it is not possible for the small amount of acidic antigen (net charge is -8 at pH 7.5 according to Helassa[35]) to produce similarly acidic local conditions. Additionally, DIC measurements closer to neutral, at pH 3, do not show the same level of pore formation passing through the entire film, though there is some degradation. It is therefore unlikely that the small amounts (10 ng/ml in PBS) of antigen would be able to produce similarly drastic effects.

As our trityl-based side chains are extremely bulky compared to the rest of the film, it is plausible that a limited degree of acid-catalyzed cleavage and removal of the trityl groups will result in sufficient structural alteration to allow this film that is relatively stable in neutral pH to still be infiltrated by water through these openings, as shown in the bottom schematic. As the highly hydrated proteins bring additional polar water molecules to the site of the potential trityl cleavage, the reaction is additionally aided by the protonation of the carbonyl groups by COOH groups on the antigen. The resulting deprotected carboxylic acid groups on the polymer will additionally increase acidity of the system, helping to promote the process further. The areas where cleavage occurred are water soluble, and could allow for sufficient polymer flexibility to allow for further water infiltration. The resulting change in dielectric properties caused by the surrounding polar medium should be rapidly observable (within a few minutes) via electronic measurements.

Furthermore, despite the highly regular phase angle shift indicating an antigen sensing response, no similarly consistent decrease in the real portion of the complex impedance was found in our data. Were there significant pore formation through the bulk of our film, this would resemble an array of conductors in parallel, with weak polymer points being significantly less resistive. In such a case we would expect the overall impedance to decrease significantly. However, as no such shift in resistance was seen in our data, and no visible changes were noted in film quality, we must conclude that there are no large pores acting as conductive pathways through our film. However, the shift in capacitance is consistent with an increase in dielectric constant of our film (measured at a typical 4-5). This is consistent with Brasher and Kingsbury's explanation of water absorption through a polymer coating, where the addition of water with a dielectric constant closer to 80 begins to increase film capacitance before any purely resistive effects are noted.[36] This is due to the speed with which water can enter a film and diffuse, much faster than other electroactive species. Bellucci further noted that, over short timescales such as we have when the polymer film is beginning to react with the antigen of interest (1-5 minutes), resistive changes can be highly variable and are not a reliable measure to determine change in the polymer thin film.[37] SEM micrographs confirm that very small pores do form after a short period of incubation, and there is significant change in overall polymer morphology, as shown in Figure 6. This further supports our decision to examine the phase shift of our EIS data, rather than focusing on overall impedance, as well as supporting our hypothesized mechanism of action.

The fact that only the most labile polymer side chain produced an effective degradation response is consistent with the dimethoxytrityl cation being significantly more stable than monomethoxytrityl or trityl, allowing for faster cleavage. Additionally, the increased number of

methoxy groups would attract polar water molecules more strongly, allowing for better conditions for trityl bond cleavage to take place.

## 5. Conclusion

In this work, we have shown a simple method by which to create a series of trityl-based methacrylates and their respective co-polymers, which are capable of acting as sufficiently stable dielectric layers for use in electrochemical detection systems. Dimethoxytrityl (as well as the more stable monomethoxytrityl and trityl protecting groups) are sufficiently stable under anhydrous conditions to form copolymers with benzyl methacrylate. Additionally, these polymers show a level of acid-lability caused by their fragile side chains, which leads to a morphological change in the thin film as seen by both DIC and electrochemical impedance spectroscopy.

These polymers can be blended with a related polymer containing carboxylic acid groups capable of being bound to antibodies through carbodiimide attachment chemistry, and the thin films are resistant to non-specific binding as shown by fluorescent microscopy. These polymers are also highly promising binding layers for use in development of EIS-based sensors due to their apparently consistent capacitive changes following antigen attachment, which do not require any additional label or processing steps to produce a signal. The films are also non-reactive to other proteins such as BSA, even at a very high concentration of 10 mg/ml, and retain their ability to react as expected with our antigen of interest even in the presence of this other protein.

**Conflict of interests statement:** There are no conflicts of interest to declare.

**References**

1       M. Varshney and Y. Li, *Biosens. Bioelectron.*, 2009, **24**, 2951–2960.

2       M. Varshney and Y. Li, *Biosens. Bioelectron.*, 2007, **22**, 2408–2414.

3       F. Lisdat and D. Schäfer, *Anal. Bioanal. Chem.*, 2008, **391**, 1555–1567.

4       T. C. Hang and A. Guiseppi-Elie, *Biosens. Bioelectron.*, 2004, **19**, 1537–1548.

5       E. Silbergeld, *Chickenizing Farms and Food*, Johns Hopkins Press, 2016.

6       Scientific Advisory Group on Antimi and Scientific Advisory Group on Antimicrobials of the Committee for Medicinal Products for Veterinary Use, , DOI:10.1111/j.1365-2885.2009.01075.x.

7       F. J. Angulo, N. L. Baker, S. J. Olsen, A. Anderson and T. J. Barrett, *Semin. Pediatr. Infect. Dis.*, 2004, 15, 78–85.

8       R. C. Neyra, J. Frisancho, J. Rinsky, C. Resnick, K. Carroll, A. Rule, T. Ross, Y. You, L. Price and E. Silbergeld, *Environ. Health Perspect.*

9       C. Cuny, L. Wieler and W. Witte, *Antibiotics*, 2015, **4**, 521–543.

10      L. B. Price, M. Stegger, H. Hasman, M. Aziz, J. Larsen, P. S. Andersen, T. Pearson, A. E. Waters, J. T. Foster, J. Schupp, J. Gillece, E. Driebe, C. M. Liu, B. Springer, I. Zdovc, A. Battisti, A. Franco, J. Zmudzki, S. Schwarz, P. Butaye, E. Jouy, C. Pomba, M. C. Porrero, R. Ruimy, T. C. Smith, D. A. Robinson, J. S. Weese, C. S. Arriola, F. Yu, F. Laurent, P. Keim, R. Skov and F. M. Aarestrup, *MBio*, 2012, **3**, 1–6.

11      J. L. Rinsky, M. Nadimpalli, S. Wing, D. Hall, D. Baron, L. B. Price, J. Larsen, M.

Stegger, J. Stewart and C. D. Heaney, *PLoS One*, 2013, **8**, 1–11.

12    B. Pejcic and R. De Marco, *Electrochim. Acta*, 2006, **51**, 6217–6229.

13    A. Ramanavicius, A. Finkelsteinas, H. Cesiulis and A. Ramanaviciene, *Bioelectrochemistry*, 2010, **79**, 11–16.

14    Y. Han, 2006.

15    R. Ahmed and K. Reifsnider, *Int. J. Electrochem. Sci.*, 2011, **6**, 1159–1174.

16    O. A. Sadik, A. O. Aluoch and A. Zhou, *Biosens. Bioelectron.*, 2009, **24**, 2749–2765.

17    Y. Zhou, C.-W. Chiu and H. Liang, *Sensors (Basel).*, 2012, **12**, 15036–62.

18    Y. Binti, Y. Supervised and K. Nakazato, .

19    A. Amirudin and D. Thierry, *Prog. Org. Coatings*, 1995, **26**, 1–28.

20    Y. Ben Amor, E. M. M. Sutter, H. Takenouti, M. E. Orazem and B. Tribollet, *J. Electrochem. Soc.*, 2014, **161**, 573–579.

21    C. Sumner, S. Krause and C. McNeil, *Biosens Bioelectron*, 2001, **16**, 709–714.

22    C. J. McNeil, D. Athey, M. Ball, W. O. Ho, S. Krause, R. D. Armstrong, J. Des Wright and K. Rawson, *Anal. Chem.*, 1995, **67**, 3928–3935.

23    H. Yuki, K. Hatada, T. Niinomi and Y. Kikuchi, *Polym. J.*, 1970, **1**, 36–45.

24    Y. Okamoto, K. Suzuki, K. Ohta, K. Hatada and H. Yuki, *J. Am. Chem. Soc.*, 1979, **101**, 4763–4765.

25    Y. Okamoto, S. Nakashima, K. Ohta, K. Hatada and H. Yuki, *J. Polym. Sci. Polym. Lett. Ed.*, 1975, **13**, 273–277.

26    O. J. Alley, E. Plunkett, T. S. Kale, X. Guo, G. McClintock, M. Bhupathiraju, B. J. Kirby, D. H. Reich and H. E. Katz, *Macromolecules*, 2016, **49**, 3478–3489.

27    B. Popov, M. Alwohaibi and R. White, *J. Electrochem. Soc.*, 1993, 947–951.

28    W. Huang, K. Besar, R. LeCover, P. Dulloor, J. Sinha, J. F. Martínez Hardigree, C. Pick, J. Swavola, A. D. Everett, J. Frechette, M. Bevan and H. E. Katz, *Chem. Sci.*, 2014, **5**, 416.

29    F. Buth, A. Donner, M. Sachsenhauser, M. Stutzmann and J. a Garrido, *Adv. Mater.*, 2012, **24**, 4511–7.

30    A. B. Kharitonov, M. Zayats, A. Lichtenstein, E. Katz and I. Willner, *Sensors Actuators, B Chem.*, 2000, **70**, 222–231.

31    H. U. Khan, M. E. Roberts, O. Johnson, R. Förch, W. Knoll and Z. Bao, *Adv. Mater.*, 2010, **22**, 4452–6.

32    I. Zaccari, A. G. Davies, C. Walti and S. X. Laurenson, *Proc. 7th Cairo Int. Biomed. Eng. Conf.*

33    B. O. Fraser-Reid, K. Tatsuta and J. (Joachim) Thiem, *Glycoscience : chemistry and*

*chemical biology I-III*, Springer, 2001.

34    J. Song, J. Dailey, H. Li, H.-J. Jang, P. Zhang, J. Wang, A. D. Everett and H. E. Katz, *Adv. Funct. Mater.*

35    N. Helassa, W. Vollmer, E. Breukink, T. Vernet and A. Zapun, *FEBS J.*, 2012, **279**, 2071–2081.

36    D. M. Brasher and A. H. Kingsbury, *J. Appl. Chem.*, 2007, **4**, 62–72.

37    F. Bellucci, M. Valentino, T. Monetta, L. Nicodemo, J. Kenny, L. Nicolais and J. Mijovic, *J. Polym. Sci. Part B Polym. Phys.*, 1994, **32**, 2519–2527.

# Impedance Spectroscopic Detection of Binding and Reactions in Acid-Labile Dielectric Polymers for Biosensor Applications

Jennifer Dailey[1], Michelangelo Fichera[1], Ellen Silbergeld[2], Howard Katz[1]

[1] Department of Materials Science and Engineering, Whiting School of Engineering, Johns Hopkins University

[2] Department of Environmental Engineering, School of Public Health, Johns Hopkins University